J Bioenerg Biomembr (2008) 40:485–492
DOI 10.1007/s10863-008-9180-8

The road to the crystal structure of the cytochrome bc_1 complex from the anoxigenic, photosynthetic bacterium *Rhodobacter sphaeroides*

Di Xia · Lothar Esser · Maria Elberry · Fei Zhou · Linda Yu · Chang-An Yu

Received: 11 July 2008 / Accepted: 1 August 2008 / Published online: 25 October 2008

Abstract The advantages of using bacterial systems to study the mechanism and function of cytochrome bc_1 complexes do not extend readily to their structural investigations. High quality crystals of bacterial complexes have been difficult to obtain despite the enzymes' smaller sizes and simpler subunit compositions compared to their mitochondrial counterparts. In the course of the structure determination of the bc_1 complex from *R. sphaeroides*, we observed that the growth of only low quality crystals correlated with low activity and stability of the purified complex, which was mitigated in part by introducing a double mutations to the enzyme. The S287R(cyt *b*)/V135S (ISP) mutant shows 40% increase in electron transfer activity and displays a 4.3 °C increase in thermal stability over wild-type enzyme. The amino acid histidine was found important in maintaining structural integrity of the bacterial complex, while the respiratory inhibitors such as stigmatellin are required for immobilization of the iron-sulfur protein extrinsic domain. Crystal quality of the *R. sphaeroides* bc_1 complex can be improved further by the presence of strontium ions yielding crystals that diffracted X-rays to better than 2.3 Å resolution. The improved crystal quality can be understood in terms of participation of strontium ions in molecular packing arrangement in crystal.

D. Xia (✉) · L. Esser
Laboratory of Cell Biology, Center for Cancer Research,
National Cancer Institute, National Institutes of Health,
Bethesda, MD 20892, USA
e-mail: dixia@helix.nih.gov

M. Elberry · F. Zhou · L. Yu · C.-A. Yu (✉)
Department of Biochemistry and Molecular Biology,
Oklahoma State University,
Stillwater, OK 74078, USA
e-mail: cayu@okstate.edu

Abbreviations

bc_1 complex	ubiquinol-cytochrome *c* oxidoreductase
b_H	high potential cytochrome *b* heme
b_L	low potential cytochrome *b* heme
$Btbc_1$	*Bos taurus* bc_1
cyt	cytochrome
DSC	differential scanning calorimetry
ET	electron transfer
ISP	Rieske iron-sulfur protein subunit
ISP-ED	ISP extrinsic domain
PDC	protein-detergent complex
PEG	polyethylene glycol
MR	molecular replacement
[2Fe-2S]	Rieske iron-sulfur center
SMC	sucrose monocaprate

Introduction

The cytochrome bc_1 complex (cyt bc_1 or bc_1), also known as ubiquinol cytochrome *c* oxidoreductase, is a multi-subunit integral membrane protein that constitutes an essential component of the cellular respiratory chain; It catalyzes electron transfer from ubiquinol to cyt *c* coupled with proton translocation across the membrane (Trumpower and Gennis 1994). The cross-membrane electrochemical gradient is used as an energy source to generate ATP by ATP synthase. Subunit compositions of bc_1 complexes vary depending on organisms ranging from three subunits in *P. denitrificans* and *R. capsulatus* (Yang and Trumpower 1986; Robertson et al. 1993) to as many as eleven subunits, as in bovine mitochondria (Schagger et al. 1995). Three redox subunits are essential and are found in all species; they are cyt *b* housing hemes b_L and b_H, cyt c_1 containing a

heme *c* and the Iron sulfur protein (ISP) featuring a 2Fe-2S cluster (Trumpower 1990; Mitchell 1976). All additional subunits, referred to as supernumerary subunits, are believed to contribute to the increased stability of the protein (Ljungdahl et al. 1987; Yu et al. 1999). Despite its size (500 kDa for the dimer) and complexity (11 different subunits in a monomer), crystal structures for the bovine mitochondrial cyt bc_1 complex (*Bos taurus* bc_1, $Btbc_1$) were determined first (Xia et al. 1997; Esser et al. 2004; Huang et al. 2005). The bc_1 complex isolated from *R. sphaeroides* ($Rsbc_1$), on the other hand, has been defying crystallization efforts until very recently (Elberry et al. 2006), even though it is smaller in size (250 kDa per dimer) due to its much simpler composition having only one supermumerary subunit: subunit IV (Yu et al. 1999). The simpler subunit composition, amenable to genetic manipulations, and easy to express and purify in large quantity make the $Rsbc_1$ an excellent model of the mitochondrial complex and an ideal system for investigating into the mechanism of bc_1 function. Indeed, most of the structural information obtained from the mitochondrial enzyme has been validated via molecular genetic manipulations of the bacterial enzyme. Although the structures of the bacterial and mitochondrial complexes were expected to be very similar, an experimental structure of the bacterial bc_1 was highly desirable due to sequence variations and numerous insertions and deletions in the bacterial sequences.

Despite its simple composition and small size, the structure determination of $Rsbc_1$ had been hampered by poor crystal qualities, a problem also apparent in the structure from *R. capsulatus* (Berry et al. 2004). As it is common in membrane protein crystallization, a number of factors could affect the diffraction quality of $Rsbc_1$ crystals. Firstly, the considerably larger proportion of hydrophobic surface compared to mitochondrial complexes limits the amount of hydrophilic interactions that are essential for crystal contacts, pointing to a more challenging crystallization case. Secondly, compared to mitochondrial enzymes, purified $Rsbc_1$ has significantly lower electron transfer (ET) activity, which are correlated to complex stability and ultimately to crystal quality. Furthermore, structures of the $Btbc_1$ revealed a highly mobile iron-sulfur protein extrinsic domain (ISP-ED), whose rapid motion is required for function as demonstrated experimentally (Esser et al. 2006; Tian et al. 1998; Darrouzet et al. 2000). In this report, we demonstrate that by carefully monitoring $Rsbc_1$ activity and structural stability, complex monodispersity, and conformational uniformity in solution, we found

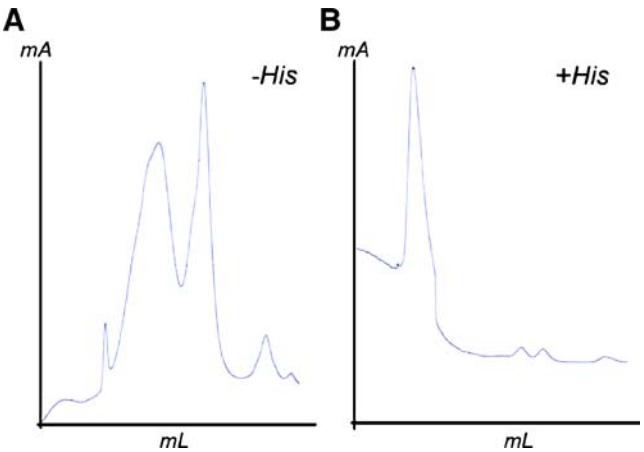

Fig. 1 Requirement of histidine for the structural integrity of $Rsbc_1$ complex. **A** Gel-filtration chromatograph of purified $Rsbc_1$ in the absence of histidine. The protein sample was run on a superdex 200 column (GE Health Science) with a flow rate of 0.5 ml/min in a buffer containing 50 mM MOPS, pH 8.0, 0.5% β-OG, 0.12% SMC, 200 mM NaCl and 10% glycerol. **B** Gel-filtration chromatograph of purified $Rsbc_1$ in the presence of 200 mM histidine. All other parameters are identical to (**A**)

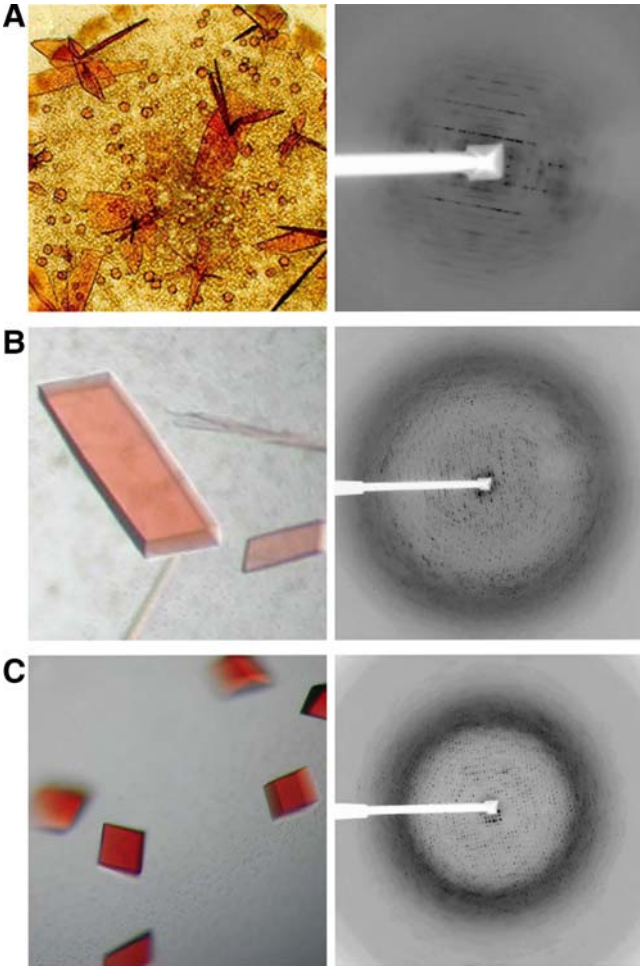

Fig. 2 Crystals of *R. sphaeroides* cytochrome bc_1 complex and their diffraction images at various stages of crystallization efforts. **A** Wild type $Rsbc_1$ and its anisotropic, low-resolution diffraction pattern at early stage of bc_1 crystallization. **B** Images of mutant $Rsbc_1$ crystals and its diffraction. **C** Crystals of $Rsbc_1$ mutant grown in the presence of strontium ion and its diffraction to 2.3 Å resolution

Table 1 Improvement in $Rsbc_1$ crystallization over time and properties of various $Rsbc_1$ crystals

Protein sample	Year	Q_N site inhibitor	Second detergent	Metal ion	No. dimmer per AU	Resolution (Å)	SG[a]	Cell parameters *a, b, c, α, β, γ (Å, °)*	PDB code
Wild type	2000	None	None	None	–	8	*P6*	–	–
Double mutant[b]	2004	None	SMC	Sr^{2+}	3	3.2	*C2*	351.3, 147.1, 160.8, 90, 103.9, 90	2FYN[c]
Double mutant	2004	UQ_2[d]	SMC	Sr^{2+}	3	2.8	*C2*	353.4, 147.1, 182.3, 90, 104.5, 90	–
ΔSub4-mutant	2005	Ant[e]	SMC	Sr^{2+}	2	3.0	*P1*	128.9, 127.0, 127.9, 64.65, 87.71, 61.80	–
Double mutant	2005	Ant	Cymal-6	Sr^{2+}	3	3.1	*C2*	352.3, 147.4, 160.8, 90, 104.1, 90	2QJK
Double mutant	2005	UQ_2	SMC	Sr^{2+}	3	2.35	*C2*	352.2, 147.2, 161.5, 90, 104.2,90	2QJY
Wild type	2006	Ant	SMC	Sr^{2+}	2	2.6	$P2_1$	135.1, 146.5, 141.0, 90, 110.2, 90	2QJP

All crystallization conditions include three- to five-fold molar excess of stigmatellin, which binds at the Q_P site
[a] Space group
[b] $Rsbc_1$ contains two mutations: S287R in cyt *b* and V135S in ISP
[c] Coordinates that have been deposited
[d] Quinone derivative with two isoprenoid repeats
[e] Antimycin A

conditions that led to the reproducible crystallization of this membrane protein complex and to well-diffracting crystals up to 2.35 Å resolution.

The requirement of histidine for complex integrity and monodispersity

Recombinant wild-type $Rsbc_1$ can be over-expressed in and purified from the *R. sphaeroides* strain BC17 bearing a plasmid pRKD*fbc*FBC$_{6H}$Q; the $Rsbc_1$ thus obtained has a his-tag at the C-terminus of the cyt c_1 subunit for easy purification by affinity chromatography (Tian et al. 1997). Initially, during purification, the elution profiles from a Ni-NTA column showed a long trailing peak when the bound $Rsbc_1$ was eluted with imidazole. This problem was solved when imidazole was replaced by the amino acid histidine in the elution buffer. In subsequent gel filtration experiments, it was found that in the absence of histidine, the protein complex had a tendency to fall apart, whereas 200 mM of histidine maintained the subunit integrity of the $Rsbc_1$ in solution (Fig. 1). In an attempt to improve the quality of the resulting crystals, we tried to replace histidine in the crystallization buffer by pyrazole, tetrazole, histidinole, 4-bromo-imidazole and melamine but without success. Thus, in all subsequent purification steps and crystallization trials, the buffers contained 200 mM histidine.

Achieving conformational uniformity using respiratory inhibitors

Structure solutions of cyt bc_1 from bovine and chicken mitochondria revealed a highly mobile extrinsic domain for the ISP subunit (ISP-ED), which appeared in various positions in different crystal environments (Xia et al. 1997; Iwata et al. 1998; Zhang et al. 1998; Xia et al. 1998). It was shown experimentally that movement of ISP-ED is required for the function of the bc_1 complex (Tian et al. 1998; Darrouzet et al. 2000) and could be arrested by a certain type of respiratory inhibitors such as stigmatellin or UHDBT (Esser et al. 2004; Kim et al. 1998). While functionally essential, the free movement of ISP-ED is highly undesirable during crystallization efforts. Due to its particular effectiveness in arresting ISP-ED, stigmatellin has been often used and described to be essential in the crystallization of yeast mitochondrial bc_1 (Hunte et al. 2000) and *R. capsulatus* bc_1 (Berry et al. 2004). In our initial crystallization condition, the $Rsbc_1$ protein was solubilized in a solution containing 50 mM Tris, pH 8.0, 0.5% β-OG,

Table 2 Summary of the wild type and the mutant $Rsbc_1$ characteristics

Strain	Mutation	Corresponding residue in bovine	Ps growth[a]	Enzymatic activity[b]		Protein soret/ UV ratio
				Chroma-tophore	Purified protein	
Wt	–	–	+++	2.0	2.5	1.2
Mutant	S287R (cyt b) V1335S (ISP)	N263 (cyt b) V145 (ISP)	+++	2.8	3.5	1.3

[a] Ps Growth (+++) refers to the photosynthetic growth rate of wild type cells
[b] The enzymatic activity is expressed as μmol cyt *c* reduced/min/nmoles cyt *b*

200 mM NaCl, and 200 mM histidine, was pre-incubated with stigmatellin (five-fold molar excess), and was readily crystallized by adding 4% PEG3500.

A problem of anisotropic diffraction of *Rsbc*$_1$ crystals

Despite early successes, all *Rsbc*$_1$ crystals were fragile and produced only relatively weak and highly anisotropic diffraction images (Fig. 2A, Table 1). Fundamental difficulties in crystallizing membrane proteins have their roots in the fact that crystals need to grow from a mixture of protein-detergent-complex (PDC) and detergent micelles. For membrane proteins with a relatively large hydrophilic surface such as mitochondrial *bc*$_1$, crystal contacts are often formed between polar residues, leading to Type-II crystals (Deisenhofer and Michel 1989; Ostermeier et al. 1997). In contrast, membrane proteins with small hydrophilic surfaces as exemplified by bacteriorhodopsin often pack together to form two-dimensional plane sheets, which stack in the 3rd dimension to form Type-I crystals (Deisenhofer and Michel 1989; Ostermeier et al. 1997). Based on the amount of hydrophobic surface, it is conceivable that *Rsbc*$_1$ crystals would belong to Type-I, which would be consistent with the observation that the first *Rsbc*$_1$ crystals were often hexagonal-shaped and showed better diffraction along the six-fold axis, suggesting conversely, a poor molecular packing within the plane sheets. To better the quality of *Rsbc*$_1$ crystals, molecular packing within a membrane plane-sheet as well as contacts between plane-sheets must be improved. It is conceivable that a more rigid protein would likely improve lateral packing of dimeric *bc*$_1$ molecules in the membrane plane, and by modulating sizes of detergent micelles, two-dimensional plane-sheets in a type-I crystal might be better aligned, giving rise to better quality crystals.

Engineering a highly active and stable *Rsbc*$_1$ complex

Establishing and maintaining sample stability and conformational uniformity present considerable challenges in membrane protein crystallization. However, it has been known for some time that bacterial *bc*$_1$ complexes have much lower ET activities and are less stable than their mitochondrial counterparts, presumably due to the lack of supernumerary subunits (Ljungdahl et al. 1987). Since the crystallization process often involves a prolonged incubation period, a more stable and rigid protein may be useful to improve the crystallization behavior of *Rsbc*$_1$. Similar approach has been reported in successful crystallization of homologous proteins from thermophilc organisms for their stabilities. The observed mobility of the ISP-ED and easy detachment of ISP subunit from the complex led us to

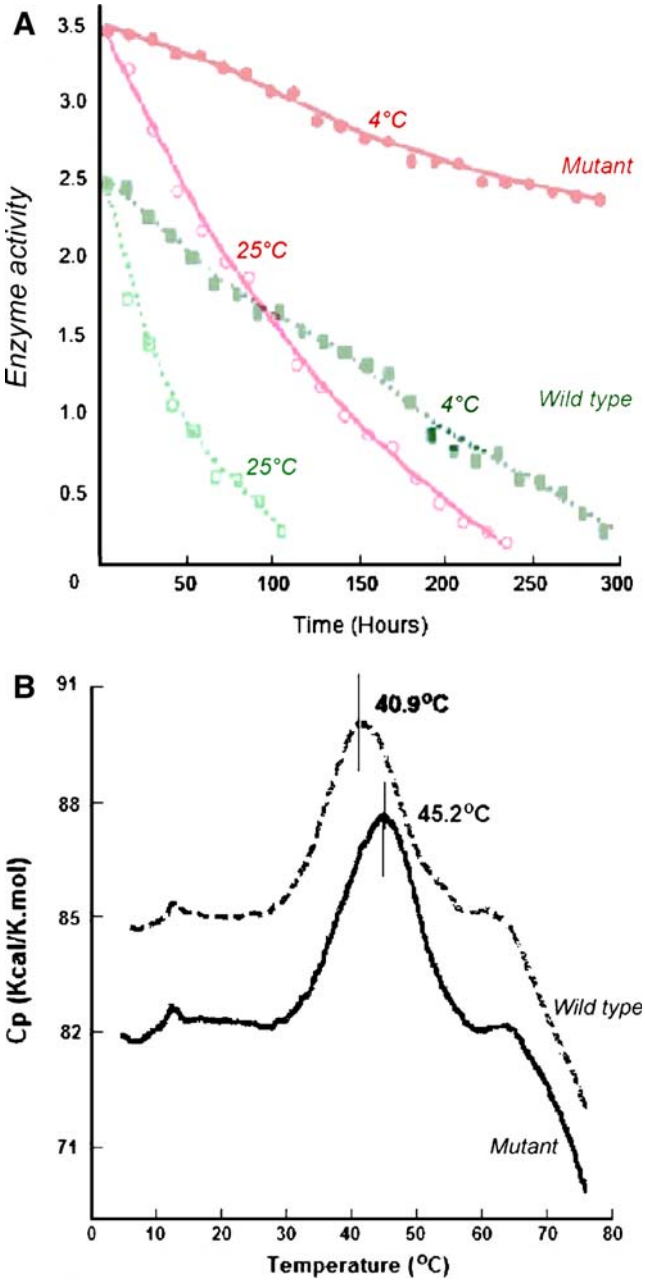

Fig. 3 Stabilities of purified cyt *bc*$_1$ complexes of wild type and mutant. **A** The enzymatic activities of wild type and mutant *Rsbc*$_1$ complexes were followed over 300 h at 4 °C and over 100 h at 25 °C, respectively. Within 4 days (100 h) of incubation at 25 °C, the wild type proteins become inactive whereas the SR mutant proteins still preserve about 50% of activity. Within 12 days (300 h) of incubation at 4 °C, the mutant proteins conserve 70% of activity as compared to nearly complete inactivation of the wild type protein. **B** Differential scanning calorimetric study of purified cyt *bc*$_1$ complexes. The thermo-denaturation temperature of the wild type (*dashed line*) and mutant (*solid line*) cyt *bc*$_1$ complex is 45.2 °C and 40.9 °C, respectively. Purified protein (0.55 mL of 15 μM cyt *bc*$_1$ complex from wild type or mutant) was subjected to differential scanning calorimetry

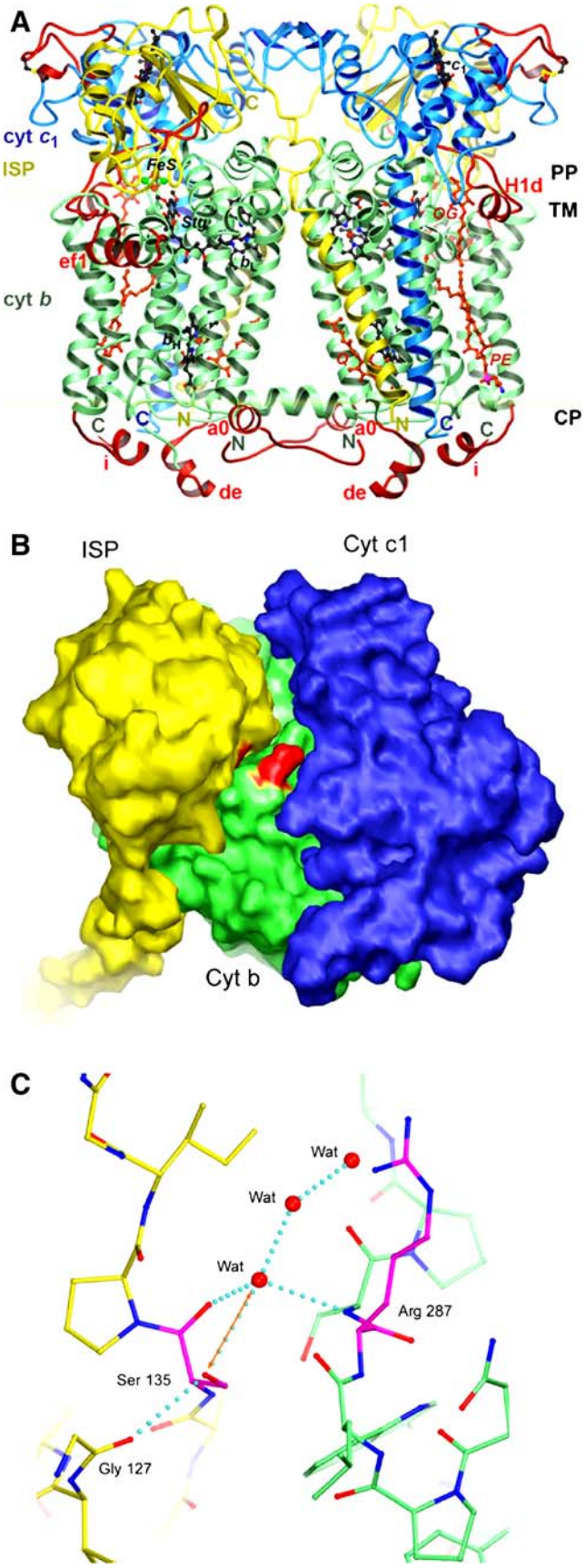

Fig. 4 Structures of the wild type and mutant three-subunit $Rsbc_1$ **A** Structure of the dimeric $Rsbc_1$ in ribbon representation with the bound Q_P site inhibitor stigmatellin and Q_N site substrate ubiquinone. Color assignment is the following: *green*, cyt *b*; *blue*, cyt c_1 and *yellow*, ISP. The insertions and extensions that distinguish $Rsbc_1$ from its mitochondrial counterpart are colored in *red*. Prosthetic groups and stigmatellin are shown as the ball-and-stick models with carbon atoms colored in *black*, oxygen *red*, nitrogen *blue*, sulfur *green* and iron *brown*. Modeled lipid and detergent molecules are shown as the ball-and-stick models in *red*. The boundary of lipid bilayer is indicated with the two parallel lines. The trans-membrane domain (*TM*), the periplasmic (*PP*) and cytoplasmic (*CP*) space are also labeled. **B** Surface diagram of the three-subunit $Rsbc_1$ shows the cyt *b* subunit in *green*, cyt c_1 in *blue* and ISP in *yellow*. The two mutations are highlighted in *red* located at the interface. **C** Stick model showing interactions at the mutation site. Carbon atoms from residues in the ISP subunit are *yellow* and those from the cyt *b* subunit are *green*, whereas those for the two mutations are shown in *magenta*. Oxygen atoms are *red* and nitrogen *blue*. Water molecules are given as *red balls*

search for more stable mutant proteins by introducing cross interactions between subunits based on mitochondrial bc_1 structures (Xiao et al. 2000). One mutant was found bearing double mutations S287R in cyt *b* and V135S in ISP, which exhibited the expected enhancement in enzymatic activity and protein stability (Elberry et al. 2006).

The *R. sphaeroides* strain harboring the mutant bc_1 complex grows photosynthetically at a similar rate to that harboring the wild type enzyme. Interestingly, enzymatic activities in both isolated chromatophore membranes and in purified forms increased by 40%, as compared to the wild type protein (Table 2). The enhanced activity was attributed to the increase in complex stability, which was demonstrated by monitoring enzyme activities of both mutant and wild type enzymes over a prolonged period of time at different temperatures (Fig. 3A). Furthermore, subsequent differential scanning calorimetry showed an increase of ΔT_m=4.3 °C in the melting temperature for the mutant protein over the wild type enzyme (Fig. 3B).

Crystallization of $Rsbc_1$ mutant and cryo protection

The $Rsbc_1$ mutant behaved significantly better even with the crystallization conditions used for the wild type enzymes. Crystals that diffracted X-rays to a much better resolution were routinely obtained, although anisotropy in diffraction patterns persisted. High-resolution diffractions were difficult to achieve in part due to the use of cryo-protection procedure for $Rsbc_1$ crystals, which involved in step-wise soaking of cryo-protectants into crystals prior to X-ray data collection and inevitably damaged the diffraction quality of $Rsbc_1$ crystals. Screening with lower molecular weight precipitants such as polyethylene glycols (PEGs) were conducted, which are themselves cryo-protectants, and $Rsbc_1$ crystals were successfully obtained

in PEG400. Crystals grew under these conditions were frozen readily with liquid propane at liquid nitrogen temperature and diffracted X-rays to 2.9 Å resolution (Fig. 2B & Table 1).

Structure determination and crystal packing analysis

Crystals of mutant $Rsbc_1$ in complex with stigmatellin frequently have the symmetry of the space group *C*2 and have large unit cell dimensions (Table 1). The structures of $Rsbc_1$-inhibitor complexes were solved by molecular replacement (MR) method using a dimeric $Rsbc_1$ model based largely on the structure of bovine bc_1 with minor modifications. Surprisingly, only the three core subunits were present (Fig. 4A); apparently, subunit IV was lost upon crystal formation. This observation was confirmed by SDS-PAGE analysis of $Rsbc_1$ crystals, which showed no band corresponding to subunit IV but it was however present in the mother liquor (Data not shown). Crystallization with purified three-subunit $Rsbc_1$ (ΔSub4-$Rsbc_1$) was also successful under conditions similar to four-subunit $Rsbc_1$ (Table 1). The assembly of the three-subunit $Rsbc_1$ resembles closely that of the corresponding subunits in bovine mitochondrial bc_1.

Although the expected interaction between the side chains of Arg287 and Ser135 of the mutant $Rsbc_1$ is not observed, several observations from the mutant structure may explain the enhancement in stability of the mutant enzyme. The introduction of two mutations, S287R in cyt *b* and V135S in ISP, at the interface considerably alters the surface property of the enzyme in this region, rendering a more hydrophilic interface than that for the wild type enzyme (Fig. 4B). As a result, ordered water molecules are localized at the interface (Fig. 4C). These solvent molecules clearly bridge hydrogen-bonding interactions between the two subunits, providing additional stability to the complex. Additionally, the hydroxyl group of Ser135 has a potential to form a hydrogen bond with the main chain amide nitrogen atom of Arg287, thus stablilizes the complex.

As expected, the mutant $Rsbc_1$ crystals are Type-I membrane protein crystals. Three bc_1 dimers occupy the crystallographic asymmetric unit (Fig. 5A). In the crystal, dimeric bc_1 molecules are aligned side-by-side in a two-dimensional plane sheet. These sheets are then stacked on top of each other to form a three-dimensional crystal.

Overcoming anisotropic diffraction by using detergent mixtures and strontium ions as additive

We found that the directions of weak intensities in the anisotropic diffraction patterns of $Rsbc_1$ crystals are

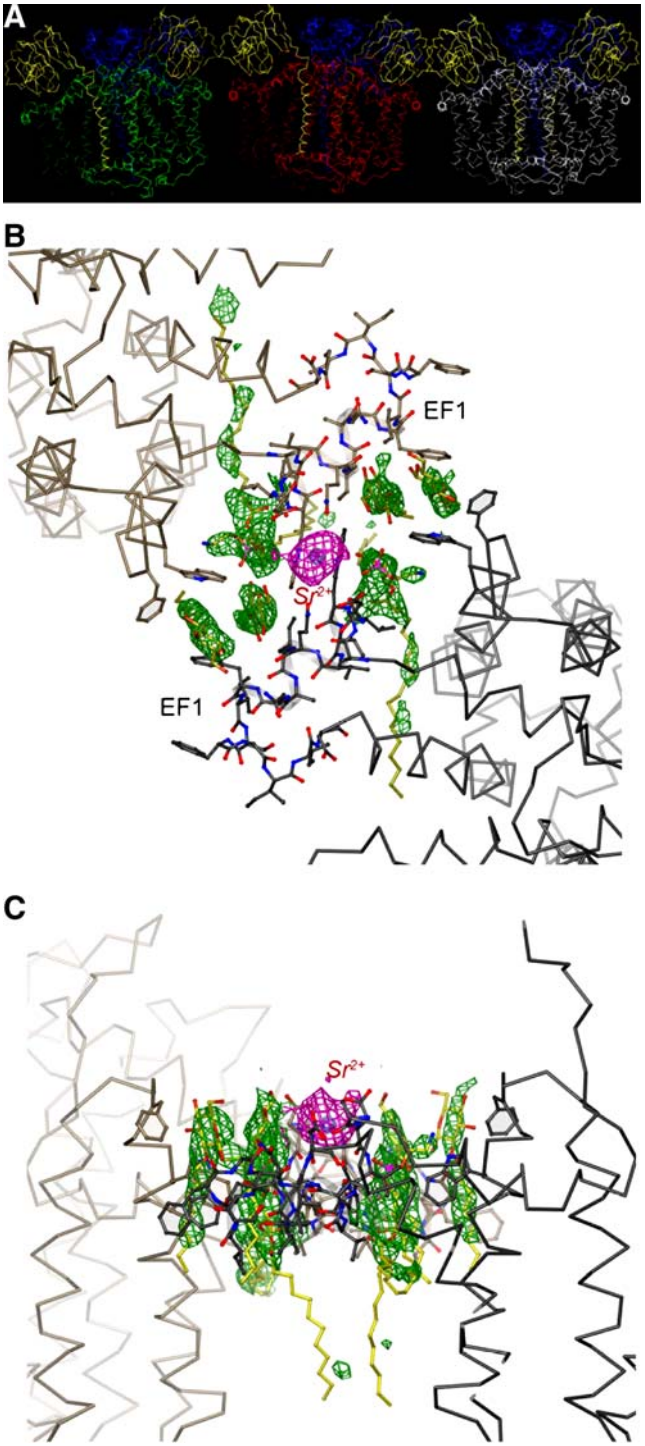

Fig. 5 Packing interactions in $Rsbc_1$ crystal **A** Packing of the three $Rsbc_1$ dimers in the asymmetric unit in the space group C2. The three independently determined dimers are shown with the three cyt *b* dimers in *green*, *red*, and *white*, respectively. The ISP subunits are *yellow* and cyt c_1 subunits *blue*. **B** Interactions at the interface between dimers mediated by Sr^{2+}. This is the view from periplasma looking down the cytoplasmic membrane. The two $Rsbc_1$ dimers contact each other through the EF1 insertion, which is unique to photosynthetic bacteria. The anomalous electron density from the Sr^{2+} ion is given in magenta, whereas the difference density shown in green are likely from bound lipid molecules. **C** The same as **B** except viewed parallel with the membrane plane

invariably associated with the packing of $Rsbc_1$ molecules in stacked two-dimensional plane sheet. To overcome the problem of anisotropic diffraction, we considered it paramount to identify conditions that would provide stronger, specific interaction between $Rsbc_1$ molecules in the adjacent two-dimensional plane sheets. We focused on the optimization of two crystallization parameters that we deemed particularly important. First, as detergent micelles may be incorporated into protein crystals, their average size and shape represent adjustable parameters. Secondly, specific interactions between neighboring molecules could be established or strengthened by metal ions—a phenomenon that has been shown previously (Guo et al. 2002). To optimize the first parameter, a detergent screen kit consisting of moret than 50 different detergents and small molecule amphiphiles at various concentrations was used for screening. The sugar based detergent sucrose mono carprate (SMC) yielded crystals with good morphology and improved diffraction quality. Next, a number of mono and multivalent metal ions was screened, which established strontium nitrate as a successful additive. In the presence of both SMC and Sr^{2+}, the $Rsbc_1$ mutant crystals diffracted X-rays to better than 2.3 Å resolution with a complete data set collected to 2.35 Å resolution (Fig. 2C, Table 1). Although it is difficult to visualize the shape and size of detergent micelles in crystals, metal irons can often be seen. In the crystal, a difference Fourier map revealed a large peak at the interface between two dimers (Fig. 5B,C). Serendipitously, the helical insertion EF1 helix (312–327) in cyt *b* found in photosynthetic bacteria promotes inter-dimer interactions supported by as of yet unidentified lipid components as well as by a strontium ion.

Crystallization of wild-type $Rsbc_1$

The purified protein at a concentration of 15 mg/ml (in 50 mM Tris–HCl buffer, pH 7.5, 0.5% β-OG, 5 mM NaN_3, 200 mM NaCl, 200 mM histidine, and 10% glycerol, 0.12% SMC, and 10 mM $Sr(NO_3)_2$) is incubated with three to five fold molar excess of stigmatellin and mixed with PEG400 to a final concentration of 8% to 10%. The mixture was allowed to stand overnight at 4 °C. A small amount of precipitate was removed by centrifugation and the clear supernatant was used for crystallization by vapor diffusion in sitting drops at 15 °C. Small, red translucent crystals appear within four to 6 weeks. Notably, this condition established first for the crystallization of mutant *R. sphaeroides* cyt bc_1 allowed us to produce wild-type $Rsbc_1$ crystals that diffracted to 2.6 Å resolution with significantly reduced anisotropy. The wild-type enzyme crystallizes with two dimers per asymmetric unit (space group $P2_1$, Table 1). The structure of the wild-type complex ($P2_1$) was solved by MR using a refined dimeric polypeptide-only model of the mutant $Rsbc_1$.

References

Berry EA, Huang L, Saechao LK, Pon NG, Valkova-Valchanova M, Daldal F (2004) X-ray structure of Rhodobacter capsulatus cytochrome bc1: comparison with its mitochondrial and chloroplast counterparts. Photosyn Res 81:251–275

Darrouzet E, Valkova-Valchanova M, Daldal F (2000) Probing the role of the Fe-S subunit hinge region during Q(o) site catalysis in Rhodobacter capsulatus bc(1) complex. Biochemistry 39:15475–15483

Deisenhofer J, Michel H (1989) The photosynthetic reaction center from the purple bacterium Rhodopseudomonas viridis. Science 245:1463–1473

Elberry M, Xiao K, Esser L, Xia D, Yu L, Yu CA (2006) Generation, characterization and crystallization of a highly active and stable cytochrome bc1 complex mutant from Rhodobacter sphaeroides. Biochim Biophys Acta 1757:835–840

Esser L, Quinn B, Li Y, Zhang M, Elberry M, Yu L, Yu CA, Xia D (2004) Crystallographic studies of quinol oxidation site inhibitors: a modified classification of inhibitors for the cytochrome bc1 complex. J Mol Biol 341:281–302

Esser L, Gong X, Yang S, Yu L, Yu CA, Xia D (2006) Surface-modulated motion switch: capture and release of iron-sulfur protein in the cytochrome bc1 complex. Proc Natl Acad Sci U S A 103:13045–13050

Guo F, Esser L, Singh SK, Maurizi MR, Xia D (2002) Crystal Structure of the heterodimeric complex of the adaptor, ClpS, with the N-domain of the AAA+Chaperone, ClpA. J Biol Chem 277:46753–46762

Huang LS, Cobessi D, Tung EY, Berry EA (2005) Binding of the respiratory chain inhibitor antimycin to the mitochondrial bc1 complex: a new crystal structure reveals an altered intramolecular hydrogen-bonding pattern. J Mol Biol 351:573–597

Hunte C, Koepke J, Lange C, Rossmanith T, Michel H (2000) Structure at 2.3 A resolution of the cytochrome bc(1) complex from the yeast Saccharomyces cerevisiae co-crystallized with an antibody Fv fragment. Structure 15:669–684

Iwata S, Lee JW, Okada K, Lee JK, Iwata M, Rasmussen B, Link TA, Ramaswamy S, Jap BK (1998) Complete structure of the 11-subunit bovine mitochondrial cytochrome bc1 complex [see comments]. Science 281:64–71

Kim H, Xia D, Yu CA, Xia JZ, Kachurin AM, Zhang L, Yu L, Deisenhofer J (1998) Inhibitor binding changes domain mobility in the iron-sulfur protein of the mitochondrial bc1 complex from bovine heart. Proc Natl Acad Sci U S A 95:8026–8033

Ljungdahl PO, Pennoyer JD, Robertson DE, Trumpower BL (1987) Purification of highly active cytochrome bc1 complexes from phylogenetically diverse species by a single chromatophaphic procedure. Biochim Biophys Acta 891:227–241

Mitchell P (1976) Possible molecular mechanisms of the protonmotive function of cytochrome systems. J Theor Biol 62:327–367

Ostermeier C, Harrenga A, Ermler U, Michel H (1997) Structure at 2.7 A resolution of the Paracoccus denitrificans two-subunit cytochrome c oxidase complexed with an antibody FV fragment. Proc Natl Acad Sci U S A 94:10547–10553

Robertson DE, Ding H, Chelminski PR, Slaughter C, Hsu J, Moomaw C, Tokito M, Daldal F, Dutton PL (1993) Hydroubiquinone-cytochyrome c2 oxidoreductase from Rhodobacter capsulatus:

definition of a minimal, functional isolated preparation. Biochemistry 9:1310–1317

Schagger H, Brandt U, Gencic S, von Jagow G (1995) Ubiquinol-cytochrome-c reductase from human and bovine mitochondria. Methods Enzymol 260:82–96

Tian H, Yu L, Mather MW, Yu CA (1997) The involvement of serine 175 and alanine 185 of cytochrome b of rhodobacter sphaeroides cytochrome bc1 complex in interaction with iron-sulfur protein. J Biol Chem 272:23722–23728

Tian H, Yu L, Mather MW, Yu CA (1998) Flexibility of the neck region of the rieske iron-sulfur protein is functionally important in the cytochrome bc1 complex. J Biol Chem 273:27953–27959

Trumpower BL (1990) The protonmotive Q cycle. Energy transduction by coupling of proton translocation to electron transfer by the cytochrome bc1 complex. J Biol Chem 265:11409–11412

Trumpower BL, Gennis RB (1994) Energy transduction by cytochrome complexes in mitochondrial and bacterial respiration: the enzymology of coupling electron transfer reactions to transmembrane proton translocation. Annu Rev Biochem 63:675–716

Xia D, Yu CA, Kim H, Xia JZ, Kachurin AM, Zhang L, Yu L, Deisenhofer J (1997) Crystal structure of the cytochrome bc1 complex from bovine heart mitochondria. Science 277:60–66

Xia D, Kim H, Yu CA, Yu L, Kachurin A, Zhang L, Deisenhofer J (1998) A novel electron transfer mechanism suggested by crystallographic studies of mitochondrial cytochrome bc1 complex. Biochem Cell Biol 76:673–679

Xiao K, Yu L, Yu CA (2000) Confirmation of the involvement of protein domain movement during the catalytic cycle of the cytochrome bc1 complex by the formation of the intersubunit disulfide bond between cytochrome b and the iron-sulfur protein. J Biol Chem 275:38597–38604

Yang X, Trumpower BL (1986) Purification of a three-subunit ubiquinol-cytochrome c oxidoreductase complex from Paracoccus denitrificans. J Biol Chem 261:12282–12289

Yu L, Tso SC, Shenoy SK, Quinn BN, Xia D (1999) The role of the supernumerary subunit of Rhodobacter sphaeroides cytochrome bc1 complex. J Bioenerg Biomembr 31:251–257

Zhang Z, Huang L, Shulmeister VM, Chi YI, Kim KK, Hung LW, Crofts AR, Berry EA, Kim SH (1998) Electron transfer by domain movement in cytochrome bc1. Nature 392:677–684